Available online at www.CivileJournal.org

# Civil Engineering Journal

(E-ISSN: 2476-3055; ISSN: 2676-6957)

Vol. 7, No. 02, February, 2021

# Structural Behavior of BubbleDeck Slab under Uniformly Distributed Load

Ali Sabah Mahdi [1*], Shatha Dehyaa Mohammed [2]

[1] *Ph.D. Student, Department of Civil Engineering, University of Baghdad, Baghdad, Iraq.*

[2] *Assistant Professor, Department of Civil Engineering, University of Baghdad, Baghdad, Iraq.*

Received 03 October 2020; Revised 10 January 2021; Accepted 28 January 2021; Published 01 February 2021

**Abstract**

In structural construction fields, reducing the overall self-weight of the structure is considered a primary objective and substantial challenge in the civil engineering field, particularly in earthquake-affected buildings and tall buildings. Different techniques were implemented to attain this goal; one of them is setting voids in a specific position through the structure, just like a voided slab or BubbleDeck slab. The main objective of this research is to study the structural behavior of BubbleDeck reinforced concrete slabs under the effect of static uniformly distributed load. The experimental program involved testing five fixed-end supported two-way solid and BubbleDeck slabs of dimensions 2500×2500× 200 mm. The considered parameters included the bubble's diameter 100 and 120 mm and the concrete volume reduction 15 and 18 %. The other parameters, which are concrete compressive strength and detail of the steel reinforcement, were identical for all the tested specimens to be $f_c' = 24\ MPa$ for the compressive strength and ($\emptyset\ 10\ @164\ mm$) for the steel reinforcement. The outcomes indicated that the ultimate load capacity for a BubbleDeck slab decreased by 15.93 and 11.5 % compared to the solid slab in case of concrete volume reductions 18 and 15 %, respectively. On the other hand, an advanced behavior, including the ultimate deflection, the absorbed energy, and the ductility factor, was achieved; the increments in these parameters were 39, 5.3, and 14.94 %, respectively.

*Keywords:* Uniformly Distributed Load; BubbleDeck Slab; Sustainable Material; Two-Way Slab.

## 1. Introduction

Basically, a slab is defined as a horizontal flat plate of parallel top and bottom surfaces. Generally, the slab supported system can be: reinforced concrete beams (commonly, it is casted monolithically with slabs), reinforced concrete walls, masonry walls, structural steel members, directly by columns, or continuously by ground. The construction technology of BubbleDeck slabs was adopted in many industrial projects nowadays, see Figure 1 [1, 2]. Jorgen Bruenig invented it in the 1990s and modified the first biaxial hollow slab (known as BubbleDeck now) in Denmark [3]. This type of technique has also spread in many countries like Malaysian, Adenan et al. 2019 [4] detected the applicability and barriers of implementation for BubbleDeck slab technology in Malaysia. The study was conducted in Selangor, Putrajaya, and Kuala Lumpur only. The collected data were questionnaires and an interview protocol. Few barriers to implementation were identified, and most of the respondents were interested in adopting this technology. In this system of the voided slab (BubbleDeck), recycled plastic hollow balls are used to eliminate the

* Corresponding author: ali.sabah@esraa.edu.com

http://dx.doi.org/10.28991/cej-2021-03091655

volume of concrete that had no significant structural effect on the solid slab so that the slab self-weight can be reduced to a significant extent (30 to 50) % concerning to the conventional solid slab; this can reduce the transferred loads to the whole building efficiently [5].

A theoretical study about the structural behavior of BubbleDeck slab was carried out by Teja et al. (2012) [6]. The solid slab was modeled as pure concrete thick shells, while the BubbleDeck slab was modeled as a layered shell. BubbleDeck slab was modeled as three layers, top and thin bottom layers of standard concrete, and one intermediate rectangular layer of hollow spheres that made from recycled high-density polyethylene (HDPE). The static analysis was performed; 10 $kN$ live load was applied upon both types of the models. The results of the FE analysis were compatible with the primary analysis and the experimental results. It was found out that the bending stresses of the BubbleDeck slab were smaller than that of the solid slab by 6.43%, BubbleDeck slab deflection was greater than that of the solid slab by 5.88% due to the slab stiffness decreasing that was caused by the entity of the hollow portions. The analysis results also showed that BubbleDeck slab's shear resistance is 60% from that of the same thickness's solid slab. The vertical reinforcement can be provided to solve this problem. The self-weight of the BubbleDeck slab was found to be 35% from that of the solid slab.

Pandey and Srivastava (2016) [7] performed a numerical finite element study about the structural behavior of BubbleDeck slab system of a self-weight reduction (15 %), see Figure 2, using ANSYS2000 software. The analysis results were compared with the corresponding results of a conventional deck slab system. The dimensions of the analyzed BubbleDeck slab are shown in Table 1. The analysis results showed that the ultimate moment and the internal stress of the BubbleDeck slab were greater than those of the solid deck slab by (64 %), and the deflection of the BubbleDeck is greater than that of the solid slab by (18 %) due to slab stiffness descending that occurred due to the presence of the hollow portion. The most critical static analysis results are shown in Table 2, where ($V_{13}$, $V_{23}$, $S_{max}$, and U) represented a shear force in x-z direction, shear force in y-z direction, maximum stress deck, and deflection, respectively.

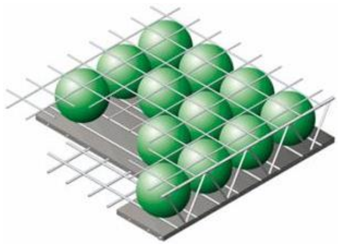

**Figure 1. BubbleDeck Slab Technology [1]**

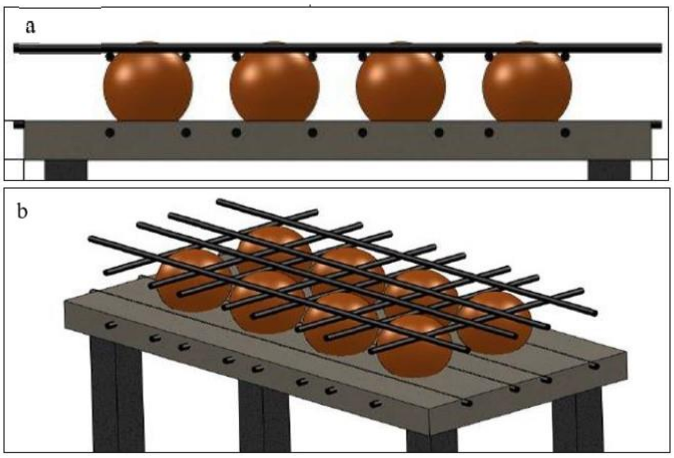


**Figure 2. BubbleDeck slab: (a) Cross-section, (b) Isometric view [7]**

**Table 1. Dimensions of BubbleDeck slab [7]**

| The Dimension of The BubbleDeck Slab | |
|---|---|
| Bubble Diameter | 6.5 cm |
| Depth | 14 cm |
| Width | 30 cm |
| Upper Concrete Thickness | 3.75 cm |
| Lower Concrete Thickness | 3.75 cm |

**Table 2. Stresses and Forces in the Solid and BubbleDeck Slabs that Resulted from Static Analysis [7]**

| | $V_{13}$ (N) | $V_{23}$ (N) | $S_{max}$ (N/cm) | U (cm) |
|---|---|---|---|---|
| **Solid deck** | -340.047 | -339.469 | 95.779 | 2.8382 |
| **BubbleDeck** | 305.896 | 305.434 | 83.289 | 3.5017 |
| **% Difference** | 10.029 | 10.029 | 13.04 | 18.2 |

Kumar and Hamza (2020) [8], conducted an analytical study about BubbleDeck slab of lightweight concrete. Four layouts of BubbleDeck slabs of identical dimensions (1400×1400×150) mm were modeled using ABAQUS Software. The models were of different spherical balls arrangement and steel reinforcement. The Finite Element Analysis (FEA) results showed that all the models were of less than 2.5% differences in load-carrying capacity. Different studies were made to investigate BubbleDeck slabs as compared to solid ones [9-14].

The experimental investigation of this research was done to study briefly the structural behavior of BubbleDeck slabs under static loading of uniformly distributed load compared to solid slab. Both concrete volume reduction (15 and 18) % and bubble diameter (100, 120) mm were taken in consideration.

## 2. Experimental Work

### 2.1. Tested Specimens

Five solid and bubbled flat two-way slabs were considered. All the specimens were (2500×2500×200) mm in length, width, and total depth, respectively, as shown in Figure 3. The specimens were designed according to ACI, 318M [15]; they were of appropriate dimensions so that the bubbles were set within the allowable spacing ($\frac{2}{3}d_{bubble}$), (Technical Manual &Documents) [16].

One of the specimens was solid slab, and the others were BubbleDeck slabs; they were divided into two groups to investigate the influence of both concrete volume reduction and bubble size upon the structural behaviour. Two bubble diameters (D1= 100 mm and D2= 120mm) and two different pairs of spacing between bubbles were adopted [(114 & 121) and (147 &160)]; a balance was made between the adopted diameters and the spacing between the bubbles so that the percentages of concrete volume reduction were differed and can be compared (R1 and R2); the groups are as follows, Table 3:

- First group: this group presents a comparison between the slabs with bubbles of similar diameters and different spacing, i.e., concrete volume reduction effect (S, B-D1-R1, and B-D1-R2) and (S, B-D2-R1, and B-D2-R2).
- Second group: this group depends mainly on comparing the slabs of different bubbles diameters and same percentages of concrete volume reduction (S, B-D1-R1, and B-D2-R1) and (S, B-D1-R2, and B-D2-R2).

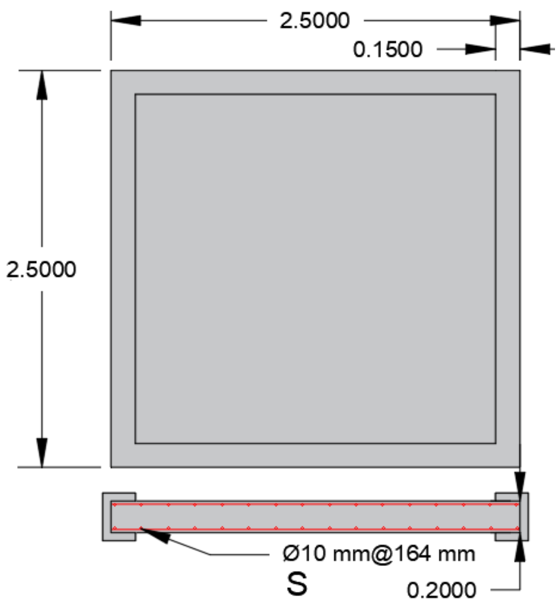

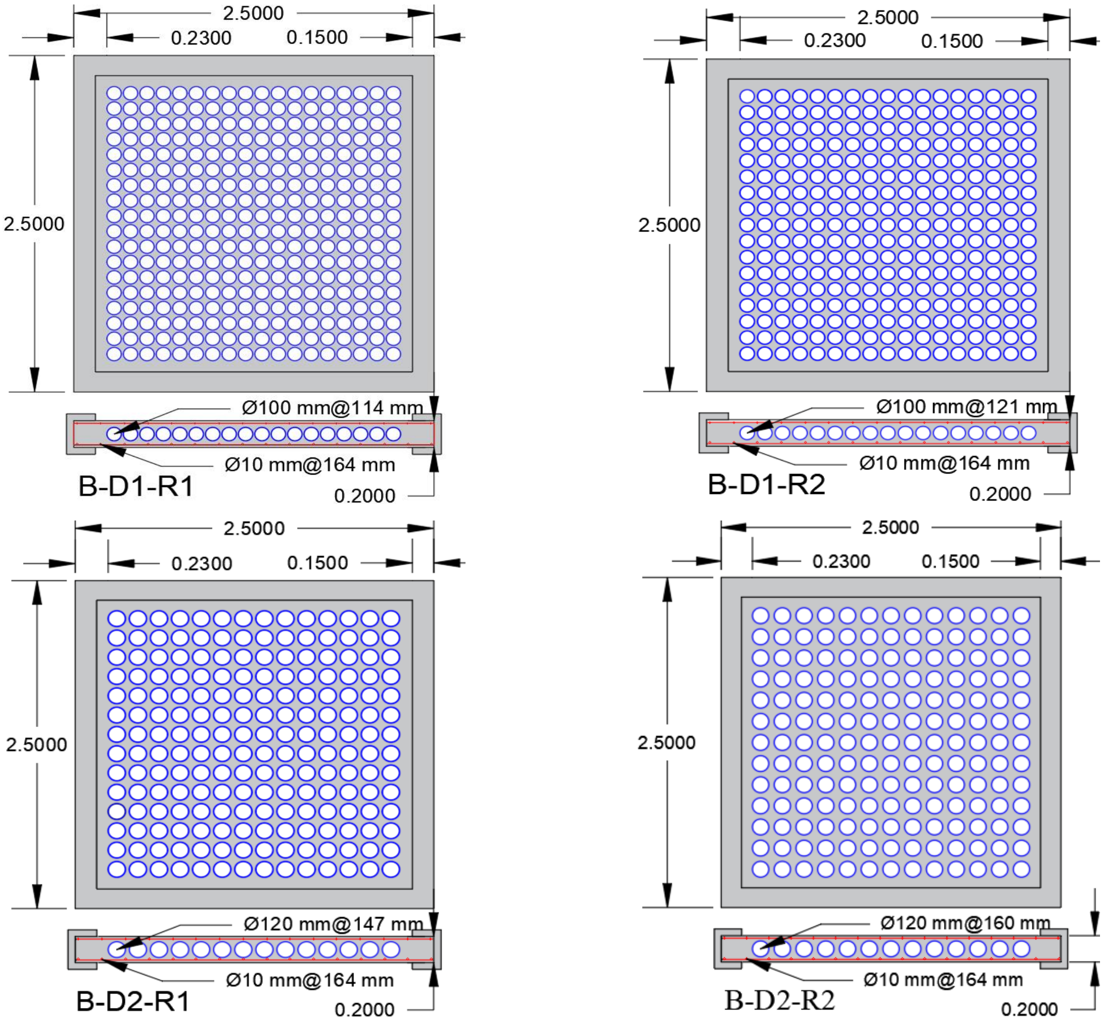


**Figure 3. Geometric layout and reinforcement details for the specimens**

**Table 3. Details of the specimens**

| Specimens designation | Slab type | Bubble diameter (mm) | Distance between bubble c/c (mm) | No. of bubble | Volume reduction % |
|---|---|---|---|---|---|
| S | Solid | - | - | - | - |
| B-D1-R1 | Bubble | 100 | 114 | 324 | 17.5 |
| B-D1-R2 | | | 121 | 289 | 15.6 |
| B-D2-R1 | | 120 | 147 | 196 | 18.4 |
| B-D2-R2 | | | 160 | 169 | 15.8 |

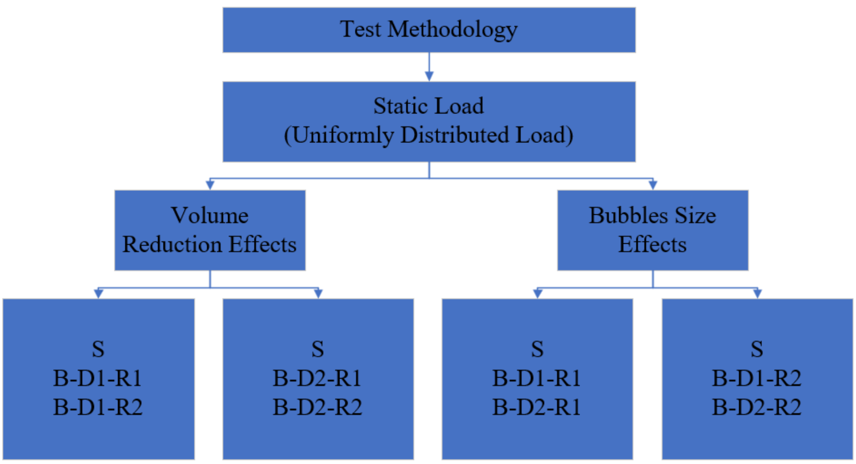


**Figure 4. Flowchart of the research methodology**

## 2.2. Materials

An ordinary Portland cement, a product of Al Qaim, was used for all the specimens. The chemical analysis and the physical test results are shown in Tables 4 and 5, respectively. The chemical and physical test results were compatible with Iraqi Specification No.5/1984 [17]. Concerning the fine aggregate, it matches with zone 2 classifications according to Iraqi Specification No. 45/1993 while crushed gravel was of (10 mm) maximum size as compared to Iraqi Specification No. 45/1993 [18]. The compressive strength used in this study was (24 MPa), trial mix according to the American standard (ACI Recommended Practice 211.1) was considered, Table 6. Deformed steel bars of 10 mm diameter were used to reinforce the specimens in both directions. Spheres of two different diameters were used (100 and 120) mm, they were manufactured in Iraq from a recycled plastic material with two rings in the top and bottom direction to facilitate the installing process by inserting a (4 mm) diameter steel bar through the upper rings for each line of spheres, and another bar was inserted through the lower ring. Then, the (4 mm) bars were linked to the upper and lower steel main reinforcement to prevent bubbles movement, Figure 5.

**Table 4. Physical properties of cement**

| Physical properties | Test result | Limit of Iraqi specification No. 5/1993 |
|---|---|---|
| Specific surface area (Blaine method), $(m^2/kg)$ | 392 | 230 min |
| **Setting time (Yicale's Method)** | | |
| The initial setting, $\boldsymbol{hrs:min}$ | 2:25 | 00:45 min |
| The final setting, $\boldsymbol{hrs:min}$ | 3.5 | 10:00 max |
| **Compressive strength (MPa)** | | |
| 7-days | 21.41 | 15.00 min |
| 28-days | 27.81 | 23.00 min |
| Autoclave Expansion % | 0.08 % | 0.8 max |

**Table 5. Chemical Composition and Main Compounds of Cement**

| Oxides Composition | Abbreviation | Content % | Limit of Iraqi Specification No. 5/1993 |
|---|---|---|---|
| Lime | $\mathrm{CaO}$ | 66.81 | - |
| Silica | $\mathrm{SiO_2}$ | 22.2 | - |
| Alumina | $\mathrm{Al_2O_3}$ | 3.73 | - |
| Iron Oxide | $\mathrm{Fe_2O_3}$ | 5.51 | - |
| Magennis | $\mathrm{MgO}$ | 2.33 | $\leq 5\%$ |
| Sulfate | $\mathrm{SO_3}$ | 2.01 | $\leq 2.8$ |
| Loss of Ignitions | L.O. I | 1.6 | $\leq 4\%$ |
| Insoluble Material | I.R | 1.27 | $\leq 1.5\%$ |
| Lime Saturation Factor | L.S. F | 0.93 | $0.66 - 1.22$ |
| Tricalcium Silicate | $\mathrm{C_3}S$ | - | - |
| Dicalcium Silicate | $\mathrm{C_2}S$ | - | - |
| Tricalcium Aluminate | $\mathrm{C_3}A$ | 0.58 | - |
| Tricalcium Alumina Ferrite | $\mathrm{C_4}AF$ | - | - |

**Table 6. Concrete Mix Design**

| Compressive strength $(\boldsymbol{MPa})$ | Cement $(\boldsymbol{kg/m^3})$ | Sand $(\boldsymbol{kg/m^3})$ | Gravel $(\boldsymbol{kg/m^3})$ | Water $(\mathbf{kg/m^3})$ |
|---|---|---|---|---|
| **24** | 420 | 630 | 1260 | 189 |


**Figure 5. a) Bubble with reinforcing steel 4mm; b) BubbleDeck Slab**

## 2.3. Test Instrumentation

An advanced digital data logger was connected to a computer device supplied by a particular program to record and save data as an excel sheet, so it is suitable for long term measurement conditions. This instrument has 24 channels divided into four groups that can read strain values with a rate of (1000 record/second) and the load capacity that’s applied on the slab, Figure 6. Two types of indicators were used to measure specimens' deflection; these are laser and LVDT indicators. The laser indicator was considered to measure the vertical deflection at the middle of the specimens, while the LVDT indicator was adopted to indicate support rotation, Figure 7.

**Figure 6. Strain Indicator**

**Figure 7. Laser indicator and LVDT indicator**

## 2.4. Uniform Load

A hydraulic jack of 150-ton capacity was used to apply the static load. The load was transferred to the slab by two steel plates, each of which was (2200×2200×300) mm attached by channels of 5 cm height extended in cross lines and welded to the lower plate; the two plates transferred the load to a layer of reinforced rubber of (4 cm thickness), and this transferred the load uniformly to the slab specimen, the load transferred system is shown in Figures 8 and 9.

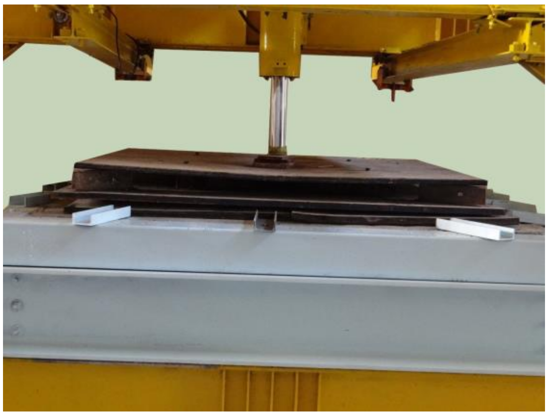

**Figure 8. Uniform load system**

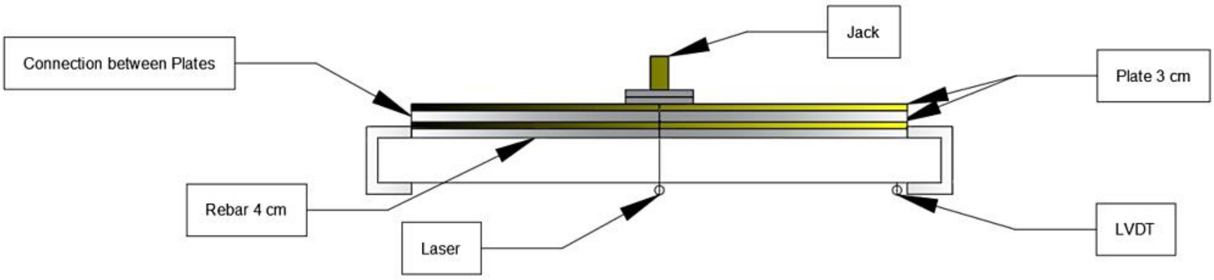


**Figure 9. A test set up**

## 3. Results and Discussion

The Cracks were initially formed at the lower face of the specimens, tension zone. Two types of cracks were recognized; the first type is the initial crack, which initiated in the early loading stage, with very small thicknesses that do not exceed (0.05 mm). The percentage of the applied load, at which this type of crack was generated, varies (10.3-18) % from the corresponding maximum carrying load capacity, as illustrated in Table 7. It was also clear for this topic that the critical specimen was represented by B-D1-R1 and B-D2-R1 in which crack load reached (10.3 and 10.5) % from the ultimate applied load, respectively. This reflected the influence of increasing concrete volume reduction on the stiffness of the specimen.

The second type of the generated cracks started and expanded along the fixed support path; this type of crack transformed the structure from statically indeterminate to statically determinate. It was detected from the recorded data that the percentage of load, which is compulsory to produce such type of cracks, varied from **(**14.7-22.1%) from the corresponding ultimate load. B-D1-R1 and B-D2-R1 represented the critical specimens as in case of initial crack, the percentage of the required load was (15.5 and 14.7%) from the maximum caring capacity load, respectively.

The closed behaviour for specimens B-D1-R1 and B-D2-R1 regarding the generation of the first and the second crack types was perceived. This can be interpreted logically because both of them have approximately the same concrete volume reduction (17.5 and 18.5%) for B-D1-R1 and B-D2-R1, respectively. As the load progressed, cracks that previously formed in the tension face of the specimens (first type) propagated and extended until they reached the slab edges and met those cracks in the supports locations as shown in (Figures 10 to 14). The width of some cracks at the final stage of loading reached (10 mm). Generally, bubbles' presence decreased load capacity of BubbleDeck slabs compared to the solid slab due to the reduction of slab stiffness, as shown in Table 7.

**Table 7. Cracked and ultimate load capacity for the specimens**

| Specimens | $P_{in-cr}$ (ton) | $P_{s-cr}$ (ton) | $P_{ul}$ (ton) | $(P_{in-cr}/P_{ul})$ % | $(Ps -_{cr}/P_{ul})$ % |
|---|---|---|---|---|---|
| S | 20 | 25 | 113 | 18 | 22.1 |
| B-D1-R1 | 10 | 15 | 97 | 10.3 | 15.5 |
| B-D1-R2 | 13 | 20.3 | 107 | 12.1 | 19 |
| B-D2-R1 | 10 | 14 | 95 | 10.5 | 14.7 |
| B-D2-R2 | 13 | 18.3 | 100 | 13 | 18.3 |

Where $P_{in-cr}$ , $P_{s-cr}$ and $P_{ul}$ ar**e** load capacity at an initial crack, support crack, and ultimate stage.


**Figure 10. A crack pattern of the specimen (S)**


**Figure 11. A crack pattern of the specimen (B-D1-R1)**


**Figure 12. A crack pattern of the specimen (B-D1-R2)**


**Figure 13. A crack pattern of the specimen (B-D2-R1)**

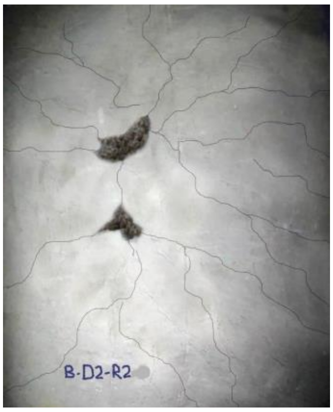


**Figure 14. A crack pattern of the specimen (B-D2-R2)**

Flexural toughness is defined as the total energy absorbed by the specimen before failure, which can be determined from the area under the load-deflection curve in flexure [10]. Table 8 shows the results of the calculated absorbed energy. The calculated energies were divided into three groups; the first one represented the absorbed energy for the specimens up to a generation of the first crack, that is to say, the absorbed energy for the phase of elastic behavior, while the second characterized the stage up to the generation of the support cracks and the last one denoted to the total absorbed energy.

Generally, it was detected that the absorbed energy for the first and second stage regarding the solid slab was more significant than that of the BubbleDeck (72.30 and 212.32) ton.mm. This fact was inversed regarding the total absorbed energy. BubbleDeck slabs tend to have absorbed energy larger than the solid ones, as shown in Table 8. This can be interpreted by the more ductile behavior of the BubbleDeck slab compared to the solid one. It was also concluded that all the BubbleDeck slabs had very close values of absorbed energy regarding the first phase (elastic behavior); the maximum variation in this stage was (5.6) %. This variation increased in the second considered phase to reach (41) % and hardly dropped down concerning the total energy (2.3) %.

The percentage of the absorbed energy up to a generation of the initial cracks to the total absorbed energy varies (0.96-2.28) % fluctuated (6.2-15.0) % up to a generation of support cracks. The Specimen B-D1-R1 and B-D2-R1 represented the most ductile behavior with total absorbed energy (3318.9 and 3328.8) ton.mm, respectively.

**Table 8. Absorb energy for the specimens**

| Specimens | Absorb energy (ton. mm) | | | | |
|---|---|---|---|---|---|
| | $E_{in-cr}$ (mm) | $E_{s-cr}$ (mm) | $E_{ul}$ (mm) | ($E_{in-cr}$ / $E_{ul}$) % | ($E_{s-cr}$ / $E_{ul}$) % |
| S | 72.30 | 212.2 | 3161.1 | 2.28 | 6.7 |
| B-D1-R1 | 32.30 | 124.2 | 3318.9 | 0.97 | 3.74 |
| B-D1-R2 | 30.50 | 190.3 | 3251.4 | 0.93 | 5.85 |
| B-D2-R1 | 32.30 | 124.4 | 3328.8 | 0.97 | 3.74 |
| B-D2-R2 | 31.20 | 186.1 | 3261.2 | 0.96 | 5.7 |

Where $E_{in-cr}$ , $E_{s-cr}$ and $E_{ul}$ are the absorb energy up to initial cracks, support cracks, and ultimate stage.

On the other hand, the angle of rotation for the fixed support was determined at yield ($\theta_y$) and ultimate stages ($\theta_U$) by installing an LVDT device at a distance (180 mm) from the fixed supports, as clearly shown in Table 9. BubbleDeck slabs trend to have a ductility factor higher than the solid slab as well these values were close to each other. The Specimen B-D2-R1 was the most ductile one since it had the highest concrete volume reduction (18.4) % and largest bubble size (120 mm), followed by specimen B-D1-R1 that had approximately the same concrete volume reduction but of smaller bubble size (100 mm), i.e., higher second moment of inertia compared to B-D2-R1. The evaluated ductility factor for both (B-D1-R2 and B-D2-R2) specimens was less than of B-D2-R1 by (2.5 and 3.5) %, respectively. This is attributed to the effect of concrete volume reduction that significantly reduced specimen's stiffness. The solid slab's ductility factor was (1.74), which presented the lowest gained value.

**Table 9. Ductility factors for the specimens**

| Specimens | $\theta_y$ (rad) | $\theta_U$ (rad) | Ductility factors |
|---|---|---|---|
| S | 0.019 | 0.033 | 1.74 |
| B-D1-R1 | 0.0224 | 0.044 | 1.96 |
| B-D1-R2 | 0.0192 | 0.037 | 1.93 |
| B-D2-R1 | 0.023 | 0.046 | 2 |
| B-D2-R2 | 0.02 | 0.039 | 1.95 |

It was observed that the recorded deflections of the BubbleDeck slabs for all the considered phases (initial crack, support crack, steel yielding, and ultimate state) reflected the effect of bubble size and concrete volume reduction; the outcomes can be divided into two pairs. The first included (B-D1-R1 and B-D2-R1) or (B-D1-R2 and B-D2-R2) specimens that reflected the effect of bubble size, while the second comprised of (B-D1-R1 and B-D1-R2) or (B-D2-R1 and B-D2-R2) specimens which showed the influence of concrete volume reduction. The concrete volume reduction had more impact upon the deflection of the specimen as compared to the solid slab. The BubbleDeck slab deflection percentage to the solid one was varied between (12.2-39) % at the ultimate stage. Regarding the critical case for deflection status, the specimens B-D1-R1 and B-D2-R1 can be considered as the most critical ones, Table 10.

**Table 10. Central deflection for the specimens**

| Specimens | $\Delta_{in-cr}$ (mm) | $\Delta_{s-cr}$ (mm) | $\Delta_{y-cr}$ (mm) | $\Delta_{ul}$ (mm) | $\Delta_{ul}/\Delta_{ul(solid)}$ (%) |
|---|---|---|---|---|---|
| S | 6.95 | 15.3 | 23.4 | 41 | - |
| B-D1-R1 | 6.42 | 12.6 | 28 | 55.5 | 35.4 |
| B-D1-R2 | 4.68 | 14.6 | 24 | 46 | 12.2 |
| B-D2-R1 | 6.94 | 14.6 | 28.6 | 57 | 39 |
| B-D2-R2 | 5.62 | 15.2 | 25.2 | 49 | 19.5 |

Where $\Delta_{in-cr}$ , $\Delta_{s-cr}$ , $\Delta_{y-cr}$ and $\Delta_{ul}$ are the deflection at initial cracks, support cracks, steel yielding, and ultimate stage.

Figures 15 and 16 show the effect of concrete volume reduction and bubble size on the structural behavior of BubbleDeck slab compared to a solid slab, respectively. Each of these figures included two parts (a and b) to comprise of the two considered cases of concrete volume reduction (R1 and R2) and bubble size (D1 and D2).

Three phases can be detected regarding load-deflection behavior; the first phase concerns with the elastic state. It was noticed that changing concrete volume reduction compared to the solid slab had a significant influence on the BubbleDeck slab's stiffness for the both considered bubble diameters. The Specimen (B-D2-R1) can be considered as the most critical case; the changing of its stiffness to the solid slab's stiffness was (49.93) %; this reduction can be interpreted by the combined effect of concrete volume reduction and bubble size. Compared to a solid slab, the most similar behavior was characterized by the specimen (B-D1-R2) with stiffness change reached (3.47) %, Table 11. The structural behavior regarding the load-deflection relationships for all the tested BubbleDeck slabs showed an increase in the effect of both concrete volume reduction and bubble size as the specimen became closer to the failure stage.

**Table 11. Stiffness for the specimens**

| Specimens | $K \times 10^3$ (kN/m) | Change (%) |
|---|---|---|
| S | 28.78 | ---- |
| B-D1-R1 | 15.58 | 45.87 |
| B-D1-R2 | 27.78 | 3.47 |
| B-D2-R1 | 14.41 | 49.93 |
| B-D2-R2 | 23.13 | 19.62 |

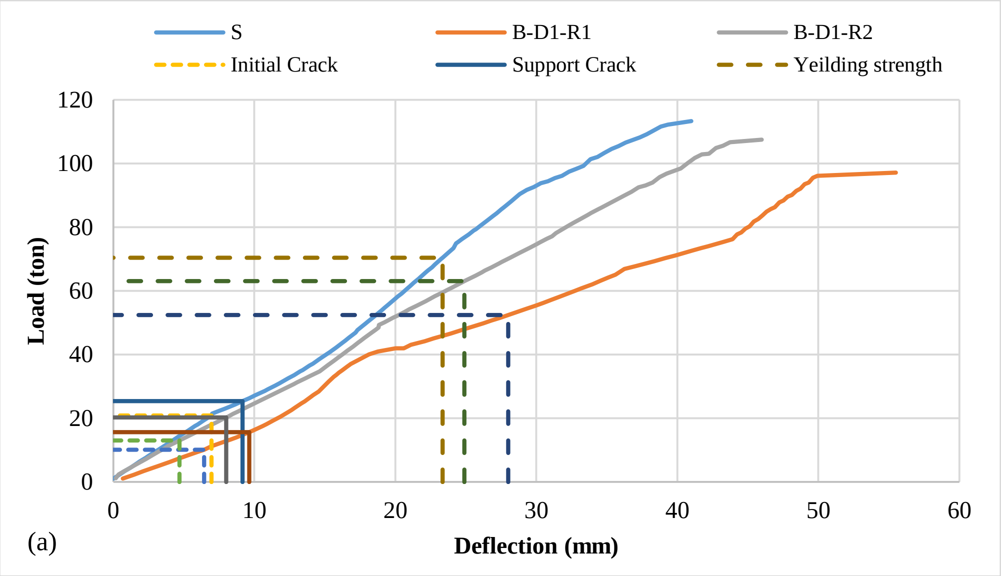


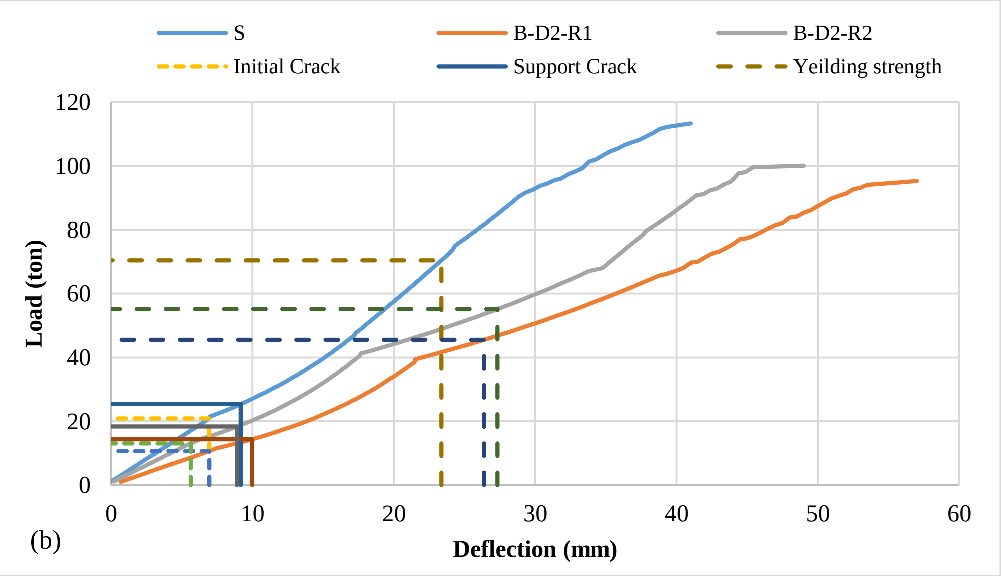


**Figure 15. Load-deflection curves for specimens of group 1 (a) Diam = 100 mm; (b) Diam = 120 mm**

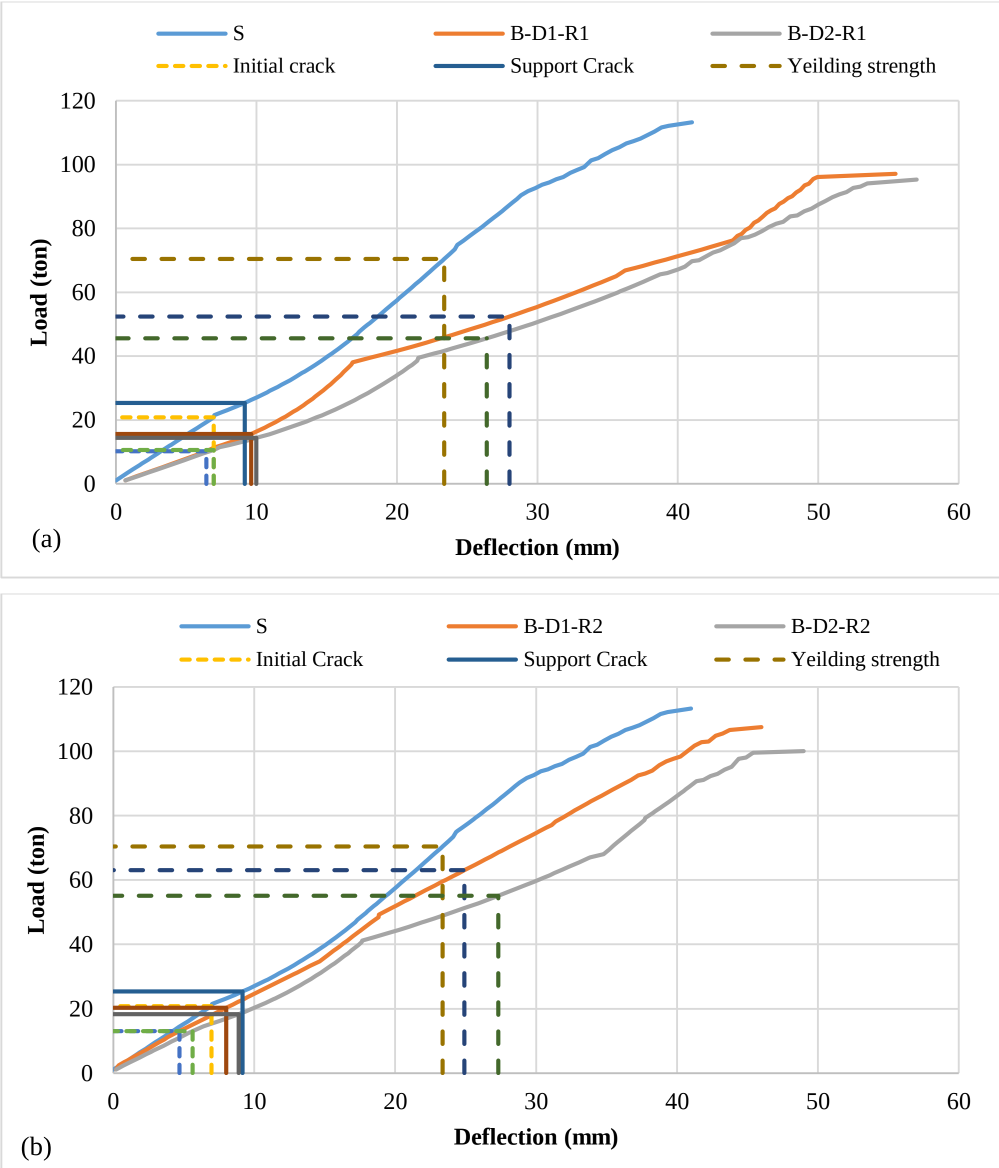


**Figure 16. Load-deflection curves for specimens of group 2 (a) Volume reduction ≈ 18%; (b) Volume reduction ≈ 15%**

Table 12 shows that the values of concrete strain at the initial crack generation stage were large for the BubbleDeck specimens compared to those of the solid one. The measured strain in this stage indicated that the specimens of less concrete volume reduction had a converged behavior rather than those of the largest concrete volume reduction as it was improved perversely, Table 12.

**Table 12. Concrete strain for the specimens**

| Specimens | $\varepsilon_{in-cr}$ (microstrain) | $\varepsilon_{s-cr}$ (microstrain) |
|---|---|---|
| S | 5.9 | 121 |
| B-D1-R1 | 63.7 | 122 |
| B-D1-R2 | 21.3 | 157 |
| B-D2-R1 | 41.8 | 155 |
| B-D2-R2 | 23.8 | 119 |

Where $\varepsilon_{in-cr}$ and $\varepsilon_{s-cr}$ are a strain at first crack, support crack.

The effect of both bubble size and concrete volume reduction upon the load-strain relationship on the concrete surface at both midpoints of the slab (tension zone) was characterized through Figures 17 and 18. The load-strain curve trend for these figures was compatible with the one of the corresponding load-deflection curves; this improved the effect of the considered parameters (bubble size and concrete volume reduction) upon the structural response of BubbleDeck slab. Lastly, the rate of change in the final stage increased rapidly, especially in the solid slab.

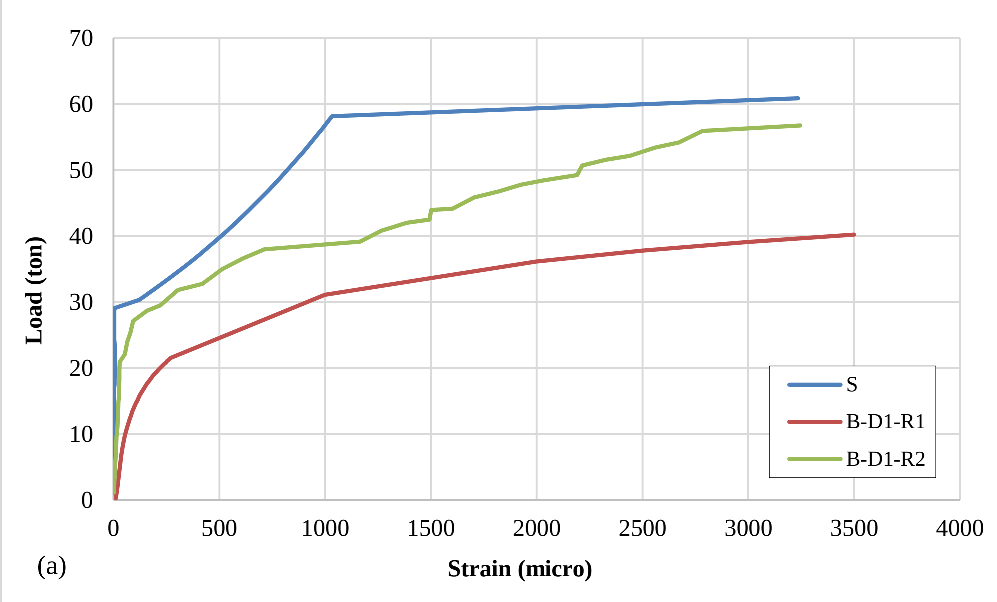


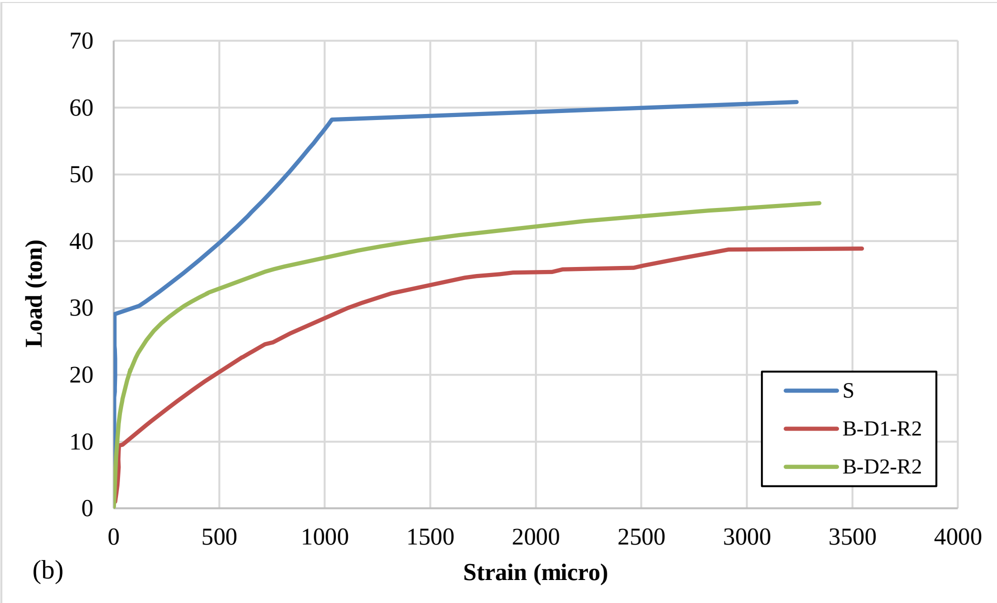


**Figure 17. Load-strain curves for specimens of group 1 (a) Diam = 100 mm; (b) Diam = 120 mm**

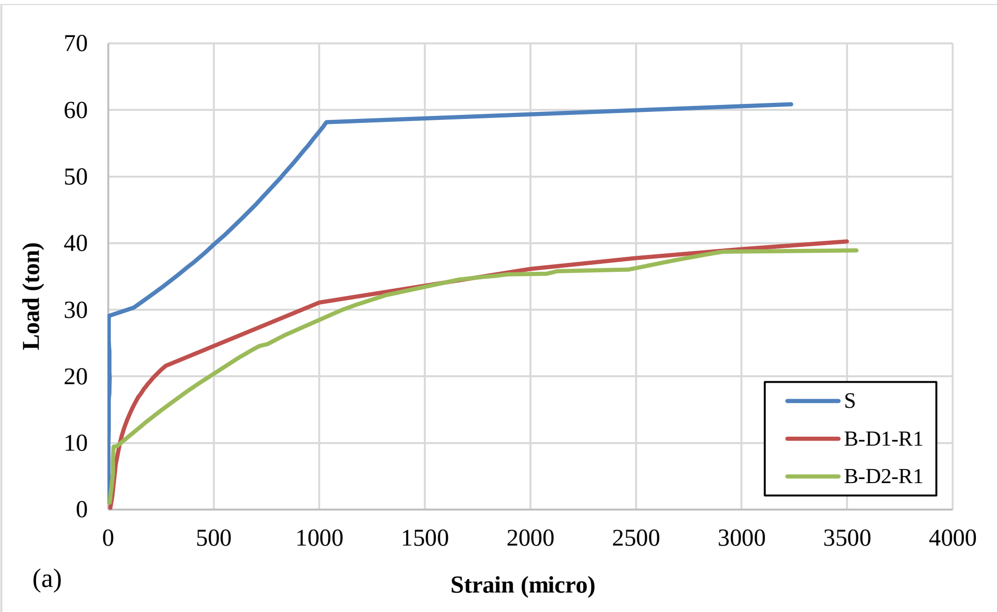

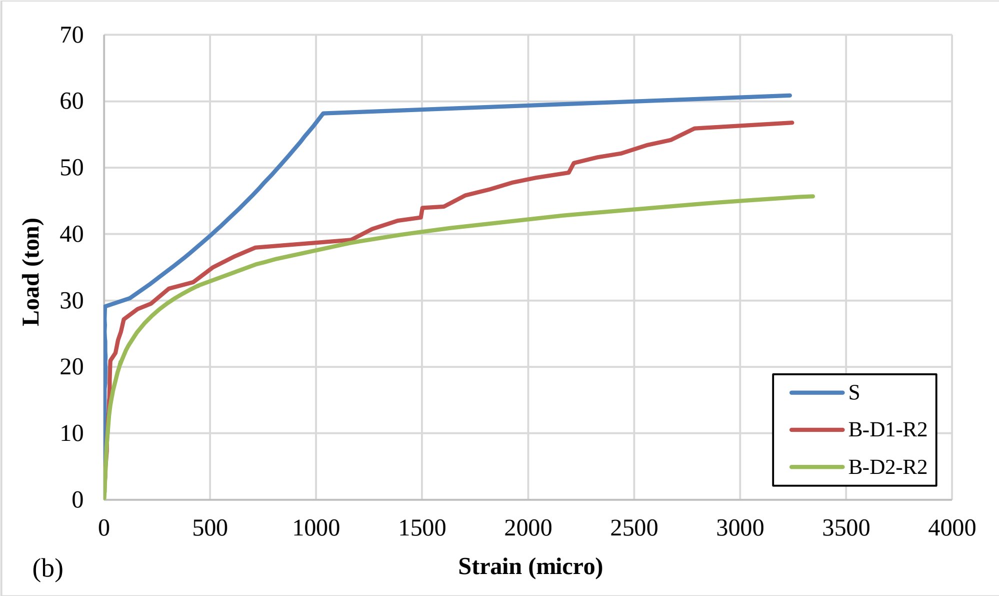


**Figure 18. Load-strain curves for specimens of group 2. (a) Volume reduction ≈ 18%; (b) Volume reduction ≈ 15 %**

From the outcomes of the strain behavior, Table 13, it can be observed that the variation in the yielding load was (10-35.7) %, corresponding to the solid slab. The Specimen (B-D2-R1) presents the critical case followed by the specimen (B-D1-R1); both present the worst-case regarding the tested BubbleDeck slabs.

**Table 13. Yielding strength in steel reinforcement**

| Specimen | Yielding strength (ton) | Changing in yielding strength (%) |
|---|---|---|
| S | 70 | - |
| B-D1-R1 | 52 | 25.7 |
| B-D1-R2 | 63 | 10 |
| B-D2-R1 | 45 | 35.7 |
| B-D2-R2 | 55 | 21.4 |

Same category was adopted to discuss both concrete volume reduction and bubble size on strain behavior. It was improved from the recorded strain outcomes that there is identical behavior between load deflection, concrete strain, and steel strain. This proves the conclusion (the specimens of the same concrete volume reduction were more compatible in their structural behavior than specimens of the same bubble size), Figures 19 and 20. A State of strain hardening was observed in the tested specimens in deflection and strain behavior, which improved the used economic design sections.

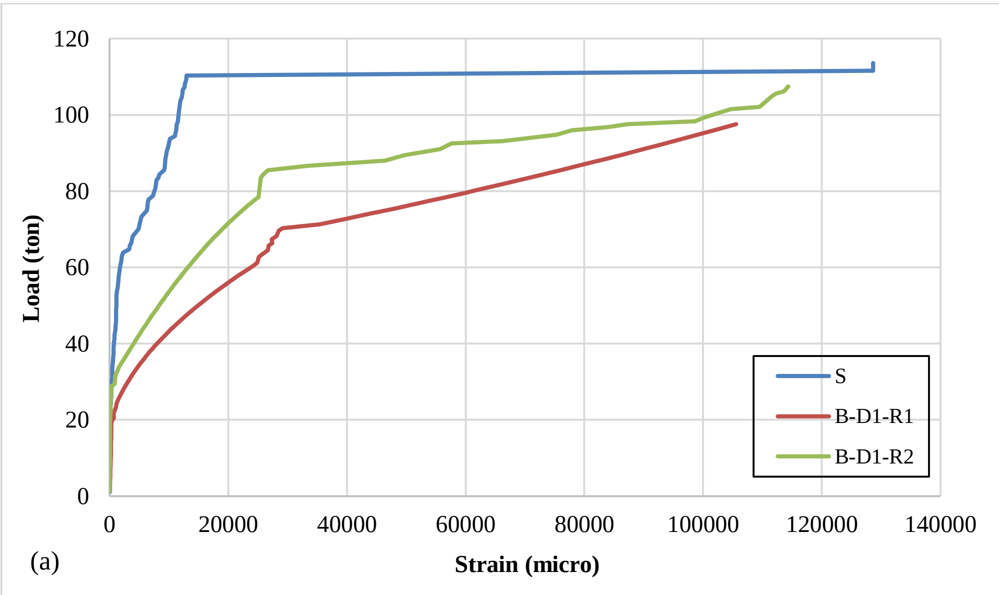

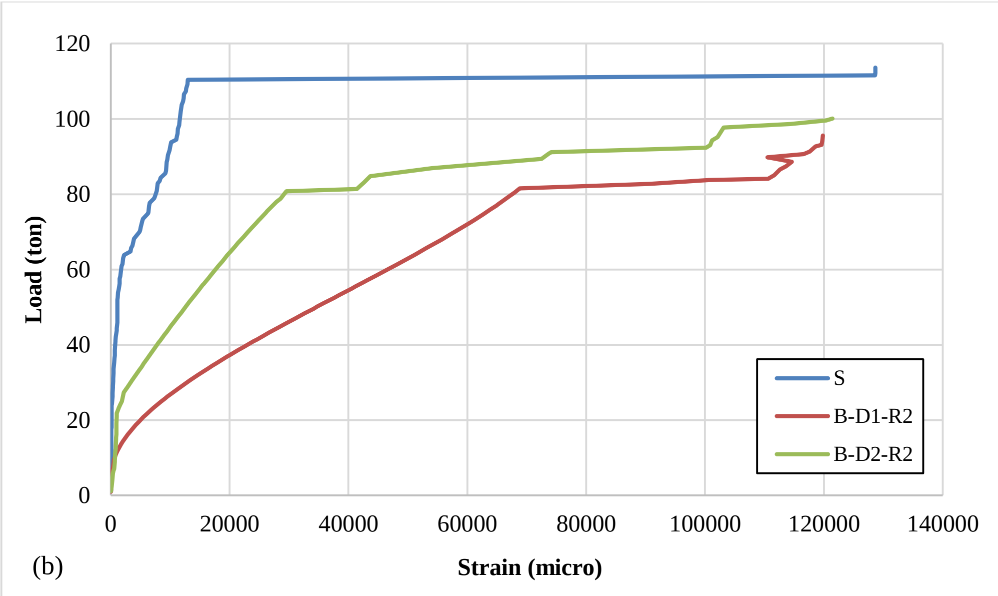


**Figure 19. Load-strain curves for specimens of group 1 (a) Diam = 100 mm; (b) Diam = 120 mm**

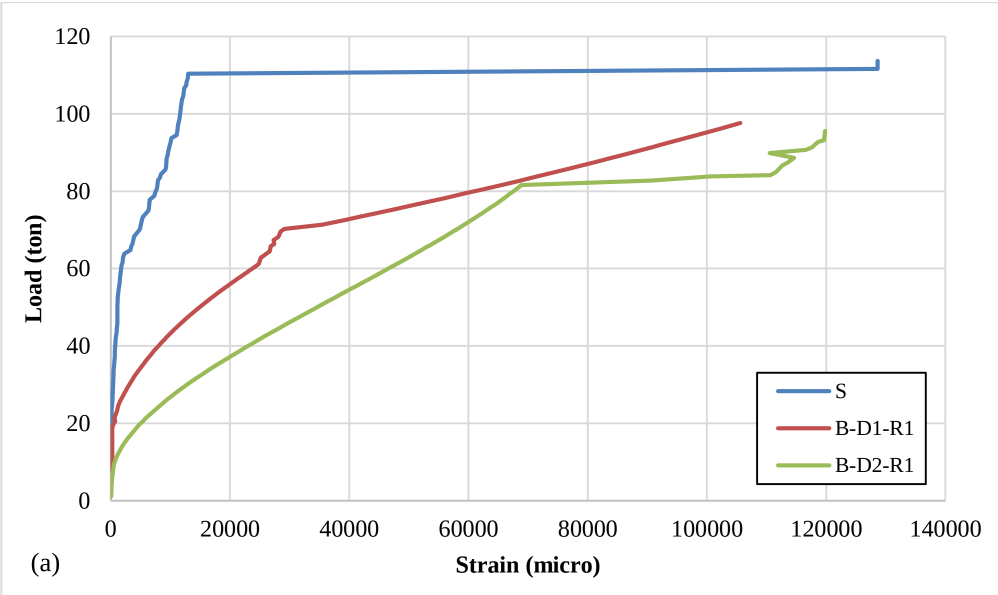


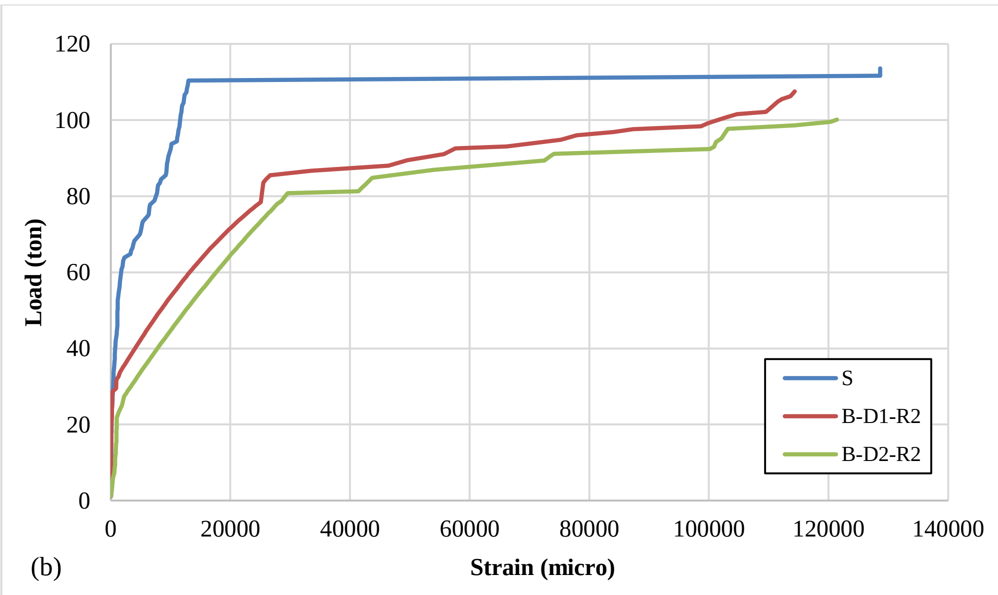


**Figure 20. Load-strain curves for specimens of group 2. (a) Volume reduction ≈ 18%; (b) Volume reduction ≈ 15 %**

# 4. Conclusions

The presence of bubbles within the slab had specific effects in comparison with the solid slab as follows:

- Decreasing the ultimate load for a solid slab by about (5.3-15.93) % where the ultimate reduction percentage (15.93 %) was corresponding to specimen of volume reduction (18.4) % and bubble diameter (120) mm;
- The absorbed energy of BubbleDeck slabs increased by about 2.86-5.3 % as compared to the solid slab;
- The Bubbles presence leads to more ductile behavior than those for the solid slab, the recorded deflection value increased by about (12.2-39) %;
- The required load that caused yielding strength in the steel reinforcement decreased by (10-35.7) %;
- BubbleDeck slabs of the comparable concrete volume reduction tend to have approximately the same structural behavior regarding ultimate load capacity, maximum deflection, and strain, although the bubble's size was different;
- The evaluated ductility factor was directly proportional to both concrete volume reduction and bubble diameter;
- A state of strain hardening was observed in the tested BubbleDeck slabs (deflection and strain behaviour), which improved the adopted bubbles distribution's economic design;
- Changing the clear spacing between bubbles of the same size had a significant influence that caused a reduction in the BubbleDeck slab's strength up to 15.9 % concerning to the solid one;
- The percentage of the initial crack load was varied between (10.3-18) % from the corresponding maximum carrying load capacity while for support cracks, it was detected that the percentage of support crack load varied from (14.7-22.1) % from the corresponding ultimate load;
- Changing concrete volume reduction compared to the solid slab had a more significant influence on the BubbleDeck slab's stiffness for both considered bubble diameters;
- The structural behaviour regarding load-deflection relationship for all the tested BubbleDeck slabs showed an increase in the effect of both concrete volume reduction and bubble size as the specimen is enclosed to the failure state.

# 5. Declarations

## 5.1. Data Availability Statement

The data presented in this study are available in article.

## 5.2. Funding

The author(s) received no financial support for the research, authorship, and/or publication of this article.

## 5.3. Conflicts of Interest

The authors declare no conflict of interest.

# 6. References

[1] Bhade, Bhagyashri G., and S. M. Barelikar. "An experimental study on two way bubble deck slab with spherical hollow balls." International Journal of Recent Scientific Research 7, no. 6 (2016): 11621-11626.

[2] Hamid, Hala Aqeel, and Shatha D. Mohammed. “Behavior of Reinforced Reactive Powder Concrete Two-Way Slabs under Static and Repeated Load.” Civil Engineering Journal 4, no. 6 (July 4, 2018): 1178. doi:10.28991/cej-0309166.

[3] Skaggs, K., “An Introduction to Bubble-Voided Concrete Flat Slabs.” The University of Cincinnati, (2017).

[4] Adenan, Dyg Siti Quraisyah Abg, Magcellia Berni, Kartini Kamaruddin, and Hamidah Mohd. "Application of the Bubble Deck Slab Technology in Malaysia." Infrastructure University Kuala Lumpur Research Journal (IUKLRJ), (2019): 43-53.

[5] Surendar, M., M. Ranjitham, and P. G. Scholar. "Numerical and experimental study on bubble deck slab." International Journal of Engineering Science and Computing 6, no. 5 (2016): 5959-5962.

[6] Teja, P. Prabhu, P. Vijay Kumar, S. Anusha, C. H. Mounika, and Purnachandra Saha. "Structural behavior of bubble deck slab." In IEEE-International Conference on Advances in Engineering, Science and Management (ICAESM-2012), pp. 383-388. IEEE, 2012.

[7] Pandey, Mrinank, and Manjesh Srivastava. "Analysis of bubble deck slab design by finite element method." IJSTE-International Journal of Science Technology and Engineering 2, no. 11 (2016): 599-606.

[8] Vinod Kumar, M, and Taha Abou Hamza. “Finite Element Analysis on Effect of Different Ball Spacing in Bubble Deck Lightweight Concrete Slab.” IOP Conference Series: Materials Science and Engineering 872 (June 27, 2020): 012124. doi:10.1088/1757-899x/872/1/012124.

[9] Hashemi, Seyed Shaker, Kabir Sadeghi, Mohammad Vaghefi, and Seyed Alireza Siadat. “Evaluation of Ductility of RC Structures Constructed with Bubble Deck System.” International Journal of Civil Engineering 16, no. 5 (February 22, 2017): 513–526. doi:10.1007/s40999-017-0158-y.

[10] Siti Quraisyah, A A Dyg, K Kartini, M S Hamidah, and K Daiana. “Bubble Deck Slab as an Innovative Biaxial Hollow Slab – A Review.” Journal of Physics: Conference Series 1711 (November 2020): 012003. doi:10.1088/1742-6596/1711/1/012003.

[11] Iswarya, M., and V. S. Tamilarasan. “Experimental Study on Bubble Deck Slab Using Palm Seeds.” Smart Technologies for Sustainable Development (October 14, 2020): 369–376. doi:10.1007/978-981-15-5001-0_31.

[12] Gao, Danying, Dong Fang, Peibo You, Gang Chen, and Jiyu Tang. “Flexural Behavior of Reinforced Concrete One-Way Slabs Strengthened via External Post-Tensioned FRP Tendons.” Engineering Structures 216 (August 2020): 110718. doi:10.1016/j.engstruct.2020.110718.

[13] Helal, Rawnaq Abbas, Haider M. Al-Baghdadi, and Nabeel Hasan Ali Al-Salim. “Using Mortar Infiltrated Fiber Concrete as Repairing Materials for Flat Slabs.” Civil Engineering Journal 6, no. 10 (October 1, 2020): 1956–1973. doi:10.28991/cej-2020-03091595.

[14] Abg Adenan, Dyg. Siti Quraisyah, K Kartini, and M. S Hamidah. “Comparative Study on Bubble Deck Slab and Conventional Reinforced Concrete Slab – A Review.” Journal of Advanced Research in Materials Science 70, no. 1 (July 15, 2020): 18–26. doi:10.37934/arms.70.1.1826.

[15] ACI, 318M. Building Code Requirements for Structural Concrete (ACI 318-19) Commentary on Building Code Requirements for Structural Concrete (ACI 318R-19).

[16] BubbleDeck Voided Flat Slab Solutions, Technical Manual and Documents, (June 2008).

[17] Iraq Standard Specification. IQS 5:84. Standard specification for Portland cement. Iraq: C.O.S.Q.C; (1984).

[18] Iraq Standard Specification. IQS 45-93. Aggregate from natural sources for concrete and building construction. Iraq: C.O.S.Q.C; (1993).